

# Folding of the Thrombin Aptamer into a G-Quadruplex with Sr<sup>2+</sup>: Stability, Heat, and Hydration

Besik I. Kankia and Luis A. Marky\*

Contribution from the Departments of Pharmaceutical Sciences and Biochemistry & Molecular Biology, University of Nebraska Medical Center, 986025 Nebraska Medical Center, Omaha, Nebraska 68198-6025

Received January 2, 2001

**Abstract:** It has been shown that the DNA aptamer d(G<sub>2</sub>T<sub>2</sub>G<sub>2</sub>TGTG<sub>2</sub>T<sub>2</sub>G<sub>2</sub>) adopts an intramolecular G-quadruplex structure in the presence of K<sup>+</sup>. Its affinity for thrombin has been associated with the inhibition of thrombin-catalyzed fibrin clot formation. In this work, we used a combination of spectroscopy, calorimetry, density, and ultrasound techniques to determine the spectral characteristics, thermodynamics, and hydration effects for the formation of G-quadruplexes with a variety of monovalent and divalent metal ions. The formation of cation–aptamer complexes is relatively fast and highly reproducible. The comparison of their CD spectra and melting profiles as a function of strand concentration shows that K<sup>+</sup>, Rb<sup>+</sup>, NH<sub>4</sub><sup>+</sup>, Sr<sup>2+</sup>, and Ba<sup>2+</sup> form intramolecular cation–aptamer complexes with transition temperatures above 25 °C. However, the cations Li<sup>+</sup>, Na<sup>+</sup>, Cs<sup>+</sup>, Mg<sup>2+</sup>, and Ca<sup>2+</sup> form weaker complexes at very low temperatures. This is consistent with the observation that metal ions with ionic radii in the range 1.3–1.5 Å fit well within the two G-quartets of the complex, while the other cations cannot. The comparison of thermodynamic unfolding profiles of the Sr<sup>2+</sup>–aptamer and K<sup>+</sup>–aptamer complexes shows that the Sr<sup>2+</sup>–aptamer complex is more stable, by ~18 °C, and unfolds with a lower endothermic heat of 8.3 kcal/mol. This is in excellent agreement with the exothermic heats of –16.8 kcal/mol and –25.7 kcal/mol for the binding of Sr<sup>2+</sup> and K<sup>+</sup> to the aptamer, respectively. Furthermore, volume and compressibility parameters of cation binding show hydration effects resulting mainly from two contributions: the dehydration of both cation and guanine atomic groups and water uptake upon the folding of a single-strand into a G-quadruplex structure.

## Introduction

The discovery of chromosomal sequences has led scientists to investigate the formation of unusual DNA structures.<sup>1</sup> Examples include telomere sequences, which are required to stabilize the ends of chromosomes for the proper replication and segregation of eukaryotic chromosomes.<sup>3</sup> These telomere ends of 12–16 bases usually have G and T repeats in one strand that overhangs at the 3' end.<sup>4</sup> Model telomere DNA sequences form a variety of tetraplex structures stabilized by cyclic hydrogen bonding of four guanines, forming G-quartets in the presence of univalent metal ions such as Na<sup>+</sup> or K<sup>+</sup>.<sup>5</sup> G-quartets are also found commonly in DNA aptamers, which have been identified by some selection process to bind specific targets.<sup>6</sup> G-quadruplexes are remarkably stable both kinetically and thermodynamically<sup>7–9</sup> because of the tight association of cations

with guanine residues.<sup>10</sup> The cations are coordinated to guanine O6 carbonyl groups between the planes of neighboring quartets. This provides a rationale for the observation that K<sup>+</sup> stabilizes such structures much more strongly than other univalent cations. Despite extensive investigations on G-quadruplexes, there is still a need to further our understanding of the role of cations in terms of their size, charge, and thermodynamic and hydration properties.

In this work, we use the oligonucleotide d(G<sub>2</sub>T<sub>2</sub>G<sub>2</sub>TGTG<sub>2</sub>T<sub>2</sub>G<sub>2</sub>), which forms an intramolecular complex with K<sup>+</sup>, as shown in Figure 1.<sup>11</sup> The complex is stabilized by two G-quartets connected by a TGT loop at the center and two T<sub>2</sub> loops.<sup>11,12</sup> This DNA aptamer binds thrombin with high-affinity and inhibits the thrombin-catalyzed fibrin clot formation.<sup>13,14</sup> Circular dichroism and melting techniques were employed to investigate the interaction of monovalent and divalent cations with this aptamer. In the presence of Rb<sup>+</sup>, NH<sub>4</sub><sup>+</sup>, Sr<sup>2+</sup>, or Ba<sup>2+</sup>, the oligonucleotide folds into stable intramolecular G-quadruplexes, similar to the one seen in the presence of K<sup>+</sup>. We have further

\* To whom all correspondence should be addressed. E-mail: lmarky@unmc.edu.

(1) Zakian, V. A. *Annu. Rev. Genet.* **1989**, *23*, 579–604. Mitas, M. *Nucleic Acids Res.* **1997**, *25*, 2245–2253.

(2) Blackburn, E. H. *Nature* **1991**, *350*, 569–573.

(3) DePamphilis, M. L. *Annu. Rev. Biochem.* **1993**, *62*, 29–63.

(4) Henderson, E. R.; Hardin, C. C.; Walk, S. K.; Tinoco, I., Jr.; Blackburn, E. H. *Cell* **1987**, *51*, 899–908. Henderson, E. R.; Blackburn, E. H. *Mol. Cell. Biol.* **1989**, *9*, 345–348.

(5) Williamson, J. R.; Raghuraman, M. K.; Cech, T. R. *Cell* **1989**, *59*, 871–880. Miura, T.; Benevides, J. M.; Thomas, G. J., Jr. *J. Mol. Biol.* **1995**, *248*, 233–238.

(6) Ellington, A. D.; Szostak, J. W. *Nature* **1990**, *346*, 818–822. Tuerk, C.; Gold, L. *Science* **1990**, *249*, 505–510.

(7) Hardin, C. C.; Henderson, E. R.; Watson, T.; Prosser, J. K. *Biochemistry* **1991**, *30*, 4460–4472. Lu, M.; Guo, Q.; Kallenbach, N. R. *Biochemistry* **1993**, *32*, 598–601.

(8) Smirnov, I.; Shafer, R. H. *Biochemistry* **2000**, *39*, 1462–1468.

(9) Chen, F.-M. *Biochemistry* **1992**, *31*, 3769–3776.

(10) Kang, C.; Zhang, X.; Ratliff, R.; Moyzis, R.; Rich, A. *Nature* **1992**, *356*, 126–131. Smith, F. W.; Feigon, J. *Nature* **1992**, *356*, 164–168. Xu, Q.; Deng, H.; Braunlin, W. H. *Biochemistry* **1993**, *32*, 13130–13137. Basu, S.; Szewczak, A. A.; Cocco, M.; Strobel, S. A. *J. Am. Chem. Soc.* **2000**, *122*, 3240–3241.

(11) Macaya, R. F.; Schultze, P.; Smith, F. W.; Roe, J. A.; Feigon, J. *Proc. Natl. Acad. Sci. U.S.A.* **1993**, *90*, 3745–3749.

(12) Schultze, P.; Macaya, R. F.; Feigon, J. *J. Mol. Biol.* **1994**, *235*, 1532–1547.

(13) Bock, L. C.; Griffin, L. C.; Latham, J. A.; Vermaas, E. H.; Toole, J. J. *Nature* **1992**, *355*, 564–566.

(14) Wang, K. Y.; Krawczyk, S. H.; Bischofberger, N.; Swaminathan, S.; Bolton, P. H. *Biochemistry* **1993**, *32*, 11285–11292.

5'-d(GGTTGGTGTGGTGG)-3'

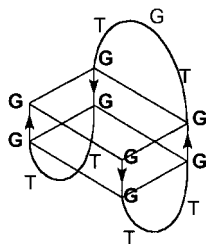


**Figure 1.** Sequence of the thrombin aptamer and its schematic structure.

characterized the thermodynamics and hydration contributions for the formation of G-quadruplexes with  $K^+$  and  $Sr^{2+}$ . The  $Sr^{2+}$ -aptamer complex unfolds with a higher transition temperature and lower endothermic heat, but its favorable formation (in terms of  $\Delta G^\circ$ ) is comparable to that of the  $K^+$ -aptamer complex. Furthermore, the hydration effects for the formation of these cation-aptamer complexes are explained in terms of two contributions: the release of electrostricted water from the cations and guanine O6 atomic groups and the immobilization of structural water by the G-quadruplex from folding a single strand.

## Materials and Methods

**Materials.** The oligonucleotide d(G<sub>2</sub>T<sub>2</sub>G<sub>2</sub>TGTG<sub>2</sub>T<sub>2</sub>G<sub>2</sub>) was synthesized by the Core Synthetic Facility of the Eppley Research Institute at UNMC, HPLC purified, and desalted by column chromatography using G-10 columns. The concentration of oligomer solutions was determined at 260 nm and 80 °C using a molar extinction coefficient of 146 mM<sup>-1</sup>cm<sup>-1</sup> (in strands). This value was calculated by extrapolation of the tabulated values of the dimers and monomer bases<sup>15</sup> at 25 °C to high temperatures using procedures reported earlier.<sup>16</sup> Reagent grade inorganic salts were purchased from either Fisher or Sigma and were used without further purification. All measurements were performed in a buffer solution consisting of 10 mM Cs-Hepes at pH 7.5; the ionic strength was adjusted by the addition of the appropriate salt.

**Circular Dichroism (CD).** The conformation of the cation-aptamer complexes was derived by simple inspection of their CD spectra. The CD spectra were obtained at several temperatures using an Aviv Model-202SF spectrometer (Lakewood, NJ) equipped with a peltier system for temperature control. Typically, a solution of oligonucleotide in the Cs<sup>+</sup> form was titrated with the appropriate cation solution, by stepwise addition of 3–5  $\mu$ L aliquots of this solution until no further changes in the spectrum took place. Quartz cells with 1 cm or 0.5 mm path lengths were used to confirm that the conformation of complexes remains unchanged as a function of aptamer concentration, especially at the higher concentrations used in ultrasonic and volumetric experiments.

**Temperature-Dependent UV Spectroscopy.** Absorbance versus temperature profiles (melting curves) were measured for each complex at two wavelengths, 260 and 297 nm, with a thermoelectrically controlled Perkin-Elmer Lambda-10 spectrophotometer as a function of oligomer concentration. The temperature was scanned at a heating rate of 0.5 °C/min. These melting curves allow us to measure transition temperatures,  $T_M$ , which are the midpoint temperatures of the order-disorder transition of the complexes, and van't Hoff enthalpies,  $\Delta H_{vH}$ , from analysis of the shape of the melting curves. In this analysis, a two-state approximation is used as reported earlier.<sup>17</sup> The formation of intramolecular complexes was assessed from the independency of  $T_M$  as a function of strand concentration.

**High Sensitivity Differential Scanning Calorimetry (DSC).** A Microcal (Northampton, MA) VP-DSC differential scanning calorimeter is used to measure the total heat required for the unfolding of the cation-aptamer complexes. Complete thermodynamic profiles can be obtained from a single differential scanning calorimetric experiment using the following relationships:<sup>17</sup>  $\Delta H_{cal}(T) = \int \Delta C_p dT$ ,  $\Delta S(T) = \int (\Delta C_p/T) dT$ , and  $\Delta G(T) = \int \Delta C_p dT - T \int (\Delta C_p/T) dT$ , where  $\Delta C_p$  is the anomalous heat capacity during the transition. The assumption is made that no heat capacity effects take place between the initial and final states. In addition, van't Hoff enthalpies,  $\Delta H_{vH}$ , can be evaluated from the half-width of the  $\Delta C_p$  versus  $T$  (or  $\Delta C_p$  versus  $1/T$ ) experimental curves using the two-state approximation. The comparison of model-independent enthalpies  $\Delta H_{cal}$  with  $\Delta H_{vH}$  enthalpies allows us to examine if the transition takes place in a cooperative two-state fashion and whether intermediate states and/or aggregate states are present.<sup>17,18</sup>

**Isothermal Titration Calorimetry.** A Microcal (Northampton, MA) Omega instrument was used to measure the heat evolved during complex formation as a function of the amount of titrant from the mixing of cation and aptamer solutions. Typically, 5  $\mu$ L aliquots of aptamer solution (210  $\mu$ M in strands) are used to titrate the appropriate cation solution with a concentration of 50  $\mu$ M (monovalents) or 10  $\mu$ M (divalents). In the reverse titrations, 5–10  $\mu$ L aliquots of the cation solutions were used to titrate a 36  $\mu$ M aptamer solution. These experiments were geared to measure only binding heats,  $\Delta H_{ITC}$ , from integrating and averaging the peaks of the initial injections, because the solute concentrations used in the reacting cell were greater than the inverse of the binding constant. The instrument was calibrated with a known electrical pulse, and its overall sensitivity is  $\sim 1 \mu$ cal.

**Measurement of Hydration Parameters.** The density,  $\rho$ , of all solutions was measured with an Anton Paar DMA-602 densimeter (Graz, Austria) with two microcells. The molar volume change,  $\Delta V$ , accompanying the interaction of a cation with the aptamer is calculated with the equation  $\Delta V = M_{complex}/\rho_{complex} - (M_{cation}/\rho_{cation} + M_{aptamer}/\rho_{aptamer})/(M_{cation}/\rho_{cation})C$ , where  $\rho_i$  and  $M_i$  are the density and mass of the solution for each participating species, respectively, and  $C$  is the molarity of the cation solution used as the limiting reagent. All solutions were prepared by weight using a Mettler microbalance.

Ultrasonic velocity measurements were made with a home-built instrument in the frequency range 7–8 MHz.<sup>19,20</sup> The molar increment of ultrasonic velocity,  $A$ , is defined by the relationship  $A = (U - U_0)/(U_0C)$ , where  $U$  and  $U_0$  are the ultrasonic velocities of the solution and solvent, respectively. The changes in the molar increment of ultrasonic velocity,  $\Delta A$ , are calculated with the relationship  $\Delta A = A_{complex} - A_{cation}$ . The change in the molar adiabatic compressibility,  $\Delta K_S$ , is determined from  $\Delta A$  and  $\Delta V$  using the relationship  $\Delta K_S = 2\beta_0(\Delta V - \Delta A)$ , where  $\beta_0$  is the adiabatic compressibility coefficient of the solvent. The density and ultrasonic velocity measurements were done at 20 °C ( $\pm 0.001$  °C). Special precautions were taken in these experiments to prevent sample evaporation.

**Hydration Contributions to the Volume and Compressibility Effects.** The molar volume,  $\Phi V$ , and molar adiabatic compressibility,  $\Phi K_S$ , for a solute in a dilute solution are based on the following relationships:<sup>21</sup>  $\Phi V = V_m + \Delta V_h$  and  $\Phi K_S = K_m + \Delta K_h$ . The  $V_m$  term is the molecular volume of the solute, while  $K_m$  is the molecular compressibility of this volume inaccessible to the surrounding solvent. The  $\Delta V_h$  and  $\Delta K_h$  terms are the hydration contributions. These contributions correspond to the changes in volume, and compressibility, of water around the solute molecule resulting from solute-water interactions and the void volume, or compressibility of this volume, between the solute molecule and of the surrounding water, respectively. The values of  $V_m$  and  $K_m$  for oligonucleotides, without significant inner cavities, are considered to remain constant during the course of a titration with cations.<sup>22</sup> The  $K_m$  term is actually small relative to the

(15) Cantor, C. R.; Warshow, M. M.; Shapiro, H. *Biopolymers* **1970**, *9*, 1059–1077.

(16) Marky, L. A.; Blumenfeld, K. S.; Kozlowski, S.; Breslauer, K. J. *Biopolymers* **1983**, *22*, 1247–1257.

(17) Marky, L. A.; Breslauer, K. J. *Biopolymers* **1987**, *26*, 1601–1620.

(18) Privalov, P. L.; Potekhin, S. A. *Methods Enzymol.* **1986**, *131*, 4–51.

(19) Eggers, F.; Funck, T. *Rev. Sci. Instrum.* **1973**, *44*, 969–977. Eggers, F.; Kaatz, U. *Meas. Sci. Technol.* **1996**, *7*, 1–19.

(20) Sarvazyan, A. P. *Ultrasonics* **1982**, *20*, 151–154.

(21) Shio, H.; Ogawa, T.; Yoshihashi, H. *J. Am. Chem. Soc.* **1955**, *77*, 4980–4982.

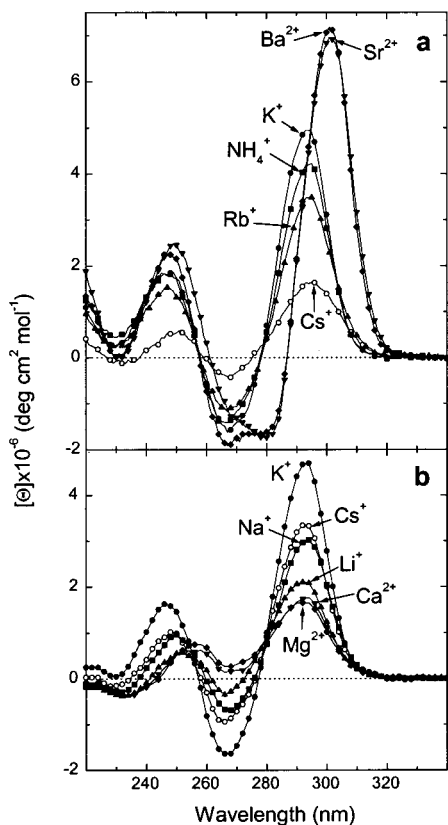


**Figure 2.** Circular dichroism spectra of d(GGTTGGTGGTGG) with different cations in 10 mM Cs–Hepes buffer at pH 7.5 and at the following temperatures: 20 °C (a) and 2 °C (b). The concentrations used are as follows: 76  $\mu$ M (oligonucleotide), 50 mM (monovalent cations), and 10 mM (divalent cations). The K<sup>+</sup> curves are included in both panels for proper comparisons.

hydration term;<sup>22</sup> therefore, the changes in  $\Phi V$  and  $\Phi K_S$  are simply a reflection of their hydration changes, that is,  $\Delta V = \Delta\Delta V_h$  and  $\Delta K_S = \Delta\Delta K_h$ .

## Results and Discussion

**Circular Dichroism Spectra and Conformation of Cation–Aptamer Complexes.** CD spectroscopy has proven to be a sensitive technique for determining the conformation of telomere model sequences. In this work, CD is used to determine the overall conformation of each cation–aptamer complex and its spectral characteristics at several temperatures. This was done in titration experiments of the oligomer in the Cs<sup>+</sup> form with each of the following cations: Li<sup>+</sup>, Na<sup>+</sup>, K<sup>+</sup>, Rb<sup>+</sup>, Cs<sup>+</sup>, NH<sub>4</sub><sup>+</sup>, Mg<sup>2+</sup>, Ba<sup>2+</sup>, Ca<sup>2+</sup>, and Sr<sup>2+</sup>. The CD spectra of the oligonucleotide saturated with each cation are shown at 20 °C and 2 °C in Figure 2a,b, respectively. The particular temperature for a given cation–aptamer complex corresponds to a temperature at which the equilibrium is shifted toward complex formation, as seen in the UV unfolding curves of the following section. The K<sup>+</sup> and Cs<sup>+</sup> curves are included in both plots for comparative purposes. Instead of the nearly conservative spectrum of the B-form with a crossover at 265 nm, all complexes have a nonconservative spectrum with a positive band centered at wavelengths  $\sim$ 290–300 nm, which characterizes the formation of antiparallel G-quartets.<sup>23</sup> The overall shape

(22) Buckin, V. A.; Kankiya, B. I.; Sarvazyan, A. P.; Uedaira, H. *Nucleic Acids Res.* **1989**, *17*, 4189–4203. Buckin, V. A.; Kankiya, B. I.; Rentzperis, D.; Marky, L. A. *J. Am. Chem. Soc.* **1994**, *116*, 9423–9429.

(23) Lu, M.; Guo, Q.; Kallenbach, N. R. *Biochemistry* **1993**, *32*, 598–601.

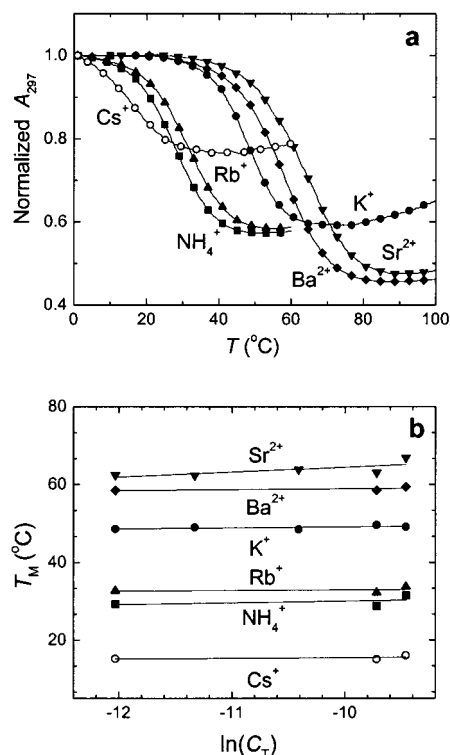


**Figure 3.** Optical unfolding of cation–aptamer complexes. (a) Typical UV melting curves in the presence of Cs<sup>+</sup>, NH<sub>4</sub><sup>+</sup>, Rb<sup>+</sup>, K<sup>+</sup>, Ba<sup>2+</sup>, and Sr<sup>2+</sup>, solution conditions as indicated in Figure 2. (b) Plots of the  $T_M$  dependence on strand concentration for each of the above cations.

of the spectra is similar, but the magnitude and location of the positive and negative bands varies with the nature of the cation. Figure 2 reveals two types of CD spectra with distinctive characteristics of the positive band at longer wavelengths. The first type with Sr<sup>2+</sup> and Ba<sup>2+</sup> shows a large band of equal magnitude centered at 300 nm, and the overall spectra for these two cations are almost superimposable. The positive band in the second type is centered at 292 nm, and its magnitude varies in the following order: K<sup>+</sup> > NH<sub>4</sub><sup>+</sup> > Rb<sup>+</sup> > Cs<sup>+</sup> > Na<sup>+</sup> > Li<sup>+</sup> > Ca<sup>2+</sup> > Mg<sup>2+</sup>. Thus, their CD spectra have a similar shape, and the magnitude of the positive band at 292 nm changes gradually. The overlay of the spectra shows an isoelliptic point at 280 nm, which indicates the formation of a similar type of complex. At 20 °C, the magnitude of the positive band of the Cs<sup>+</sup>–aptamer complex is only half the magnitude of the one at 2 °C, while for the K<sup>+</sup> complex the magnitude of this band remains the same. This shows that the Cs<sup>+</sup>–aptamer complex has unfolded to some extent. The overall spectral differences between the complexes with these monovalent and divalent ions may be attributed to differences in the coordination number of the metal ion, partial formation of complexes with some cations and/or overall tightness of each complex. Electrostatic contributions may play a role in how tightly each complex is formed, which in turn depends on both the cationic charge and ionic size.

**Unfolding of Complexes.** UV melting curves at 297 nm of the aptamer complexes in cation solutions with similar ionic strength are shown in Figure 3a. The aptamer complexes with K<sup>+</sup>, Rb<sup>+</sup>, NH<sub>4</sub><sup>+</sup>, Ba<sup>2+</sup>, and Sr<sup>2+</sup> unfold in monophasic transitions with large hypochromicities of 40–50%. The  $T_M$  values for the helix–coil transition of these complexes follow the order Sr<sup>2+</sup> (63.1 °C) > Ba<sup>2+</sup> > K<sup>+</sup> (48.7 °C)  $\gg$  Rb<sup>+</sup>  $\sim$  NH<sub>4</sub><sup>+</sup> (29 °C). On the other hand, the Cs<sup>+</sup>–aptamer complex melted with a  $T_M$  of 15 °C and a much smaller hypochromicity of  $\sim$ 23% in this short

**Table 1.** Enthalpies for the Unfolding and Formation of Cation–Aptamer Complexes<sup>a</sup>

cation	UV	DSC		ITC	
	$\Delta H_{\text{vH}}$	$\Delta H_{\text{cal}}$	$\Delta H_{\text{vH}}$	$\Delta H_{\text{ITC}}, 10\text{ }^{\circ}\text{C}$	$\Delta H_{\text{ITC}}, 20\text{ }^{\circ}\text{C}$
K <sup>+</sup>	39	25.6	36	-19.2	-24.5 (-26.0)
Rb <sup>+</sup>	35	21.6	31	-16.4	-19.6
Cs <sup>+</sup>	24	6.5	29		
NH <sub>4</sub> <sup>+</sup>	33	20.9	31	-13.2	-18.5
Sr <sup>2+</sup>	33	17.3	35	-10.2	-16.7 (-16.9)
Ba <sup>2+</sup>	34	19.1	36	-10.3	-18.5

<sup>a</sup> All values determined in 10 mM Cs–Hepes buffer containing 50 mM KCl or 10 mM SrCl<sub>2</sub>, at pH 7.5, and reported in kcal/mol. Experimental errors are given in parentheses:  $\Delta H_{\text{vH}}$  ( $\pm 15\%$ )  $\Delta H_{\text{cal}}$  ( $\pm 5\%$ ),  $\Delta H_{\text{ITC}}$  ( $\pm 4\%$ ).

temperature range, as shown in Figure 3a. It should be noted that the transition of the Cs<sup>+</sup> complex is  $\sim 70\%$  completed at 20 °C, in good agreement with the changes in ellipticity at these temperatures. The transitions with Na<sup>+</sup>, Mg<sup>2+</sup>, or Ca<sup>2+</sup> (data not shown) were similar to the Cs<sup>+</sup> transition, while a Li<sup>+</sup> transition was not observed. The UV melting curves at 260 nm (data not shown) yielded  $T_{\text{M}}$ 's in good agreement with the ones obtained at 297 nm. However, the changes in absorbance with temperature are different; for instance, the K<sup>+</sup> melting curve yielded a 6% hypochromicity, while the Sr<sup>2+</sup> curve had a 6% hyperchromicity. The melting curves at the two wavelengths of measurements are different for a given complex, because their ultraviolet spectra change differently with temperature. The main observation in these UV melts is that the  $T_{\text{M}}$  value for a given complex remains constant over a 10-fold increase in strand concentration, which confirms their intramolecular formation, as shown in Figure 3b. Model-dependent  $\Delta H_{\text{vH}}$  enthalpies, analyzed from the shape of the melting curves, are presented in the first column of Table 1. We obtained an average  $\Delta H_{\text{vH}}$  of  $35 \pm 5$  kcal/mol for the unfolding of the cation complexes with strong CD bands, while the Cs<sup>+</sup>–aptamer complex yielded a  $\Delta H_{\text{vH}}$  of  $24 \pm 5$  kcal/mol. This 35 kcal/mol value compares well with the heat of 29–40 kcal/mol for the UV unfolding of one G-quartet stack of three different telomere model sequences<sup>8,23</sup> and is significantly larger than the enthalpy value of 16 kcal/mol enthalpy for the unfolding of two GG/CC base-pair stacks, calculated from nearest neighbor parameters.<sup>24</sup>

The similarities in the CD spectral characteristics and UV melting behavior of the complexes with higher  $T_{\text{M}}$ 's indicate that Sr<sup>2+</sup>, Ba<sup>2+</sup>, K<sup>+</sup>, Rb<sup>+</sup>, and NH<sub>4</sub><sup>+</sup> induce the aptamers to fold into relative stable intramolecular G-quadruplexes. The coordination of these cations between two G-quartets correlates with the actual size of their ionic radii: K<sup>+</sup> (1.33 Å), Rb<sup>+</sup> (1.47 Å), NH<sub>4</sub><sup>+</sup> (1.43 Å), Sr<sup>2+</sup> (1.12 or 1.27 Å for a coordination number of 8), and Ba<sup>2+</sup> (1.34 Å).<sup>25</sup> This correlation indicates that an ionic radius in the range 1.3–1.5 Å is the optimum size for a cation to be sandwiched in the complex; other cations are either too small or too big.<sup>26</sup>

We have further investigated the unfolding of the stable cation–aptamer complexes using calorimetry. The corresponding DSC melting profiles are shown in Figure 4. These curves indicate that all cation–aptamer complexes unfold essentially in monophasic transitions with the exception of the complexes with Sr<sup>2+</sup> and Ba<sup>2+</sup> that showed an additional small peak at

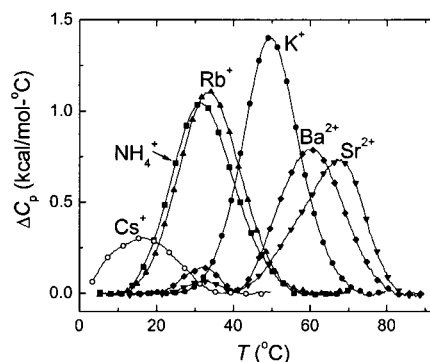


**Figure 4.** Differential scanning calorimetric curves for the unfolding of the cation–aptamer complexes. We used the following cations: Cs<sup>+</sup>, NH<sub>4</sub><sup>+</sup>, Rb<sup>+</sup>, K<sup>+</sup>, Ba<sup>2+</sup>, and Sr<sup>2+</sup> under similar solution conditions as indicated in Figure 2.

lower temperatures. The  $T_{\text{M}}$  values obtained from the peaks of these curves follow the same trend as that observed in the UV melts: Sr<sup>2+</sup> > Ba<sup>2+</sup> > K<sup>+</sup>  $\gg$  Rb<sup>+</sup>  $\sim$  NH<sub>4</sub><sup>+</sup>  $\gg$  Cs<sup>+</sup>. These  $T_{\text{M}}$  values are also included in the plots of Figure 3b and further confirm their intramolecular formation. The unfolding of complexes yielded endothermic heats in the following order: K<sup>+</sup> (25.6 kcal/mol) > Rb<sup>+</sup>  $\sim$  NH<sub>4</sub><sup>+</sup> > Ba<sup>2+</sup>  $\sim$  Sr<sup>2+</sup> (17.3 kcal/mol)  $\gg$  Cs<sup>+</sup> (6.5 kcal/mol), as shown in Table 1. The calorimetric unfolding heat for the K<sup>+</sup>–aptamer complex is in good agreement with the value of 22 kcal/mol reported previously.<sup>11</sup> Integration of the small peaks in the DSC curves of the Ba<sup>2+</sup>–aptamer and Sr<sup>2+</sup>–aptamer complexes yielded heats of 1.5 and 0.6 kcal/mol, respectively; these heats are small and may well correspond to unstacking contributions of the TGT loops. Additional peaks are not observed in the K<sup>+</sup>, Rb<sup>+</sup>, and NH<sub>4</sub><sup>+</sup> thermograms, because these complexes melt at lower temperatures and the unstacking contributions of the TGT loops may be already included in their main transitions.  $\Delta H_{\text{vH}}$  values obtained from analysis of the shape of the DSC curves are shown in the third column of Table 1. The average  $\Delta H_{\text{vH}}$  for these six cations is  $33 \pm 3$  kcal/mol, in excellent agreement with the values obtained in the optical melts. However, the  $\Delta H_{\text{vH}}$  values are much higher than the model-independent heats ( $\Delta H_{\text{cal}}$ ), as shown in Table 1. This result suggests that the unfolding of each complex is highly cooperative and consistent with the small dimensions of a cation complex with two G-quartets. An alternate and the least likely explanation for the observed  $\Delta H_{\text{vH}}/\Delta H_{\text{cal}}$  ratios of 1.4 (K<sup>+</sup>) and 2.0 (Sr<sup>2+</sup>) is the formation of aggregate states of two complex molecules, which may be consistent with the aggregation tendency of guanine residues. The Cs<sup>+</sup>–aptamer complex also unfolds with a high  $\Delta H_{\text{vH}}/\Delta H_{\text{cal}}$  ratio of 4.5, indicating that the initial state of this complex at low temperatures is a higher aggregated state.

#### Isothermal Binding Heats for the Interaction of Cation.

Isothermal titration calorimetry is used to measure the heats of complex formation at 10 °C and 20 °C. In general, the binding of a cation to the aptamer in the Cs<sup>+</sup> form is accompanied by exothermic heats. The enthalpies at 20 °C range from -24.5 kcal/mol (K<sup>+</sup>) to -16.7 kcal/mol (Sr<sup>2+</sup>), while much lower exothermic heats are obtained at 10 °C, as shown in Table 1. Their magnitude is too large to invoke solely electrostatic interactions, which are normally considered negligible;<sup>27</sup> therefore, other endothermic and exothermic contributions need to be taken into account. These endothermic contributions include

(24) Breslauer, K. J.; Frank, R.; Blocker, H.; Marky, L. A. *Proc. Natl. Acad. Sci. U.S.A.* **1986**, *83*, 3746–3750. SantaLucia, J. *Proc. Natl. Acad. Sci. U.S.A.* **1998**, *95*, 1460–1465.

(25) *CRC Handbook of Chemistry and Physics*; Weast, R., Ed.: CRC Press: Florida, 1977; F-213.

(26) Hardin, C. C.; Watson, T.; Corregan, M.; Bailey, C. *Biochemistry* **1992**, *31*, 833–841.

(27) Krakauer, H. *Biopolymers* **1972**, *11*, 811–828. Krakauer, H. *Biochemistry* **1974**, *13*, 2579–2589. Ross, P. D.; Shapiro, J. T. *Biopolymers* **1974**, *26*, 415–416.

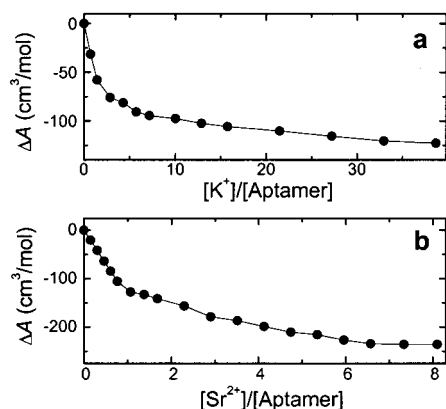


**Figure 5.** Ultrasonic titration curves of d(GGTTGGTGGTTGG) with K<sup>+</sup> (a) and Sr<sup>2+</sup> (b). All experiments done in 10 mM Cs–Hepes buffer at pH 7.5 and 20 °C. Please note that the scales of the x-axes are different.

disruption of stacking interactions of the Cs<sup>+</sup>–apptamer complex, removal of electrostricted water molecules from the cation, and the immobilization of structural water by the complex. The exothermic contributions include base stacking interactions in the formation of G-quartets upon cation binding and the removal of structural water from the existent fraction of random coils at the particular measuring temperature. The lower heats obtained in the titrations at 10 °C indicate that a higher fraction of Cs<sup>+</sup>–apptamer complex forms at this temperature; this is consistent with its unfolding transition that takes place at lower temperatures. At the same time, a higher fraction of cation–apptamer complex forms at 10 °C, as in the case of the Rb<sup>+</sup> and NH<sub>4</sub><sup>+</sup> complexes. In the titration experiments at 20 °C, the formation of the K<sup>+</sup>–apptamer, Ba<sup>2+</sup>–apptamer, and Sr<sup>2+</sup>–apptamer complexes is almost ideal, because these complexes formed completely and the Cs<sup>+</sup>–apptamer complex is ~70% disrupted. The disruption of the remaining 30% of the Cs<sup>+</sup> complex amounts to an endothermic contribution of ~2 kcal/mol. Overall, good agreement is obtained between the isothermal heats at 20 °C and the unfolding heats, as shown in Table 1, indicating negligible heat capacity effects. Furthermore, the titration experiments show that K<sup>+</sup> or Sr<sup>2+</sup> binding to the apptamer, or vice versa, yields similar exothermic heats. This indicates that these processes are in truly physical and chemical equilibrium and that aggregation of complexes can be ruled out. The average heat of these titrations yielded enthalpies of –25.7 kcal/mol and –16.8 kcal/mol for the K<sup>+</sup> and the Sr<sup>2+</sup> complexes, respectively, as shown in Table 1. Their large difference of –8.9 kcal/mol (8.3 kcal/mol if we use the calorimetric unfolding heats) suggests that K<sup>+</sup> and Sr<sup>2+</sup> have different hydration contributions. These contributions may arise from differences in both their hydration states<sup>28,29</sup> and the actual release of electrostricted water upon binding to the apptamer to form the complex.

**Hydration Parameters.** We have used density and ultrasonic techniques to determine the changes in the molar volume and molar adiabatic compressibility for the folding of complexes. The change of the concentration increment of ultrasonic velocity, ΔA, of a Cs<sup>+</sup>–apptamer solution is measured during the course of a titration with K<sup>+</sup> or Sr<sup>2+</sup>. The resulting curves are shown in Figure 5. These acoustic titration curves reveal that an increase in cation concentration is accompanied by a decrease in the increment of ultrasound velocity. The curves show an

**Table 2.** Complete Thermodynamic Profiles for the Formation of G-Quadruplexes at 20 °C<sup>a</sup>

cation	$T_M^b$	$\Delta G^\circ$	$\Delta H_{cal}^c$	$T\Delta S^c$	$\Delta H_{ITC}^c$	$\Delta V^d$	$\Delta\Phi K_S \times 10^4^e$
K <sup>+</sup>	49.1	–2.3	–25.6	–23.3	–24.5 (–26.8)	–15.9	98.5
Sr <sup>2+</sup>	66.9	–2.4	–17.3	–14.9	–16.7 (–16.9)	–15.3	108.4

<sup>a</sup> All values determined in 10 mM Cs–Hepes buffer containing 50 mM KCl or 10 mM SrCl<sub>2</sub>, at pH 7.5. The  $T_M$  ( $\pm 0.5$  °C),  $\Delta G^\circ$  ( $\pm 5\%$ ),  $\Delta H_{cal}$  ( $\pm 5\%$ ), and  $T\Delta S$  ( $\pm 7\%$ ) were determined in DSC experiments. The  $\Delta H_{ITC}$  ( $\pm 4\%$ ) values were determined in ITC experiments, while  $\Delta V$  ( $\pm 15\%$ ) and  $\Delta\Phi K_S$  ( $\pm 10\%$ ) were determined in density and ultrasonic measurements. The ITC enthalpy values in parentheses correspond to reverse titrations. <sup>b</sup> Units of °C. <sup>c</sup> Units of kcal/mol. <sup>d</sup> Units of cm<sup>3</sup>/mol. <sup>e</sup> Units of cm<sup>3</sup>/mol·bar.

initial sharp decrease of ΔA, which corresponds to complex formation, followed by a gradual leveling off. In the K<sup>+</sup> curve, the initial decrease takes place up to a [K<sup>+</sup>]/[apptamer] ratio of 3, while in the Sr<sup>2+</sup> curve the decrease occurs up to a [Sr<sup>2+</sup>]/[apptamer] ratio of 1. This indicates the formation of tighter complexes with Sr<sup>2+</sup> because of its higher charge. After these ratios, the overall changes in ΔA are small for K<sup>+</sup> and very large for Sr<sup>2+</sup> and may correspond to the hydration effects for the interaction of cations with the surface of the cation–apptamer complexes.<sup>22,30</sup>

The ΔA values obtained at [cation]/[apptamer] ratios of 1 (Sr<sup>2+</sup>) and 3 (K<sup>+</sup>), together with parallel density measurements, were used to characterize the hydration parameters that take place in the formation of the cation–apptamer complexes at 20 °C. The volume and compressibility effects for the formation of G-quadruplexes with K<sup>+</sup> and Sr<sup>2+</sup> are shown in the last two columns of Table 2. We obtained negative values for the volume change, indicating a decrease in the total volume of the system. This shows that complex formation with K<sup>+</sup> and Sr<sup>2+</sup> is accompanied by an uptake of water molecules, because the molar volume of water around a solute is considered lower than that of bulk water.<sup>31</sup> On the other hand, the changes in the molar compressibility parameter are negative, which indicate the opposite, a release of water molecules. This apparent discrepancy on the opposite signs of these two parameters invokes the participation of two types of water molecules, electrostricted (around charged atomic groups) and hydrophobic or structural (around polar and nonpolar groups), on the formation of cation–apptamer complexes. Therefore, the overall hydration effects accompanying the binding of each cation correspond to a partial conversion of electrostricted water to hydrophobic water. However, a closer look on the physical events that take place on complex formation indicates that these hydration parameters are the result of mainly two contributions: the uptake of water due to the conformational reorganization of forming a folded G-quadruplex from the random coil state (or some other form in Cs<sup>+</sup>) and the cation dehydration upon binding tightly to the quadruplex core. The hydration contribution due to the atmospheric binding of counterions is considered negligible at these particular [cation]/[apptamer ratios].<sup>22</sup> In the particular case of Sr<sup>2+</sup>, its hydration contribution can be estimated from similar parameters of its binding to EDTA where the cation loses ~80% of its hydrating water.<sup>32</sup> The volume and compressibility effects for the formation of a Sr<sup>2+</sup>–EDTA complex are 40.5 cm<sup>3</sup>/mol and  $116 \times 10^{-4}$  cm<sup>3</sup>/mol·bar, respectively,<sup>32</sup> and correspond

(30) Kankia, B. I. *Biophys. Chem.* **2000**, *84*, 227–237. Kankia, B. I. *Nucleic Acids Res.* **2000**, *28*, 911–916.

(31) Millero, F. J. In *Water and Aqueous Solutions*; Horn, R. A., Ed.; Wiley-Interscience: New York, 1972; pp 519–595. Marky, L. A.; Kupke, D. W.; Kankia, B. I. *Methods Enzymol.* **2001**, *340*, 149–165.

(32) Kankia, B. I.; Funck, T.; Uedaira, H.; Buckin, V. A. *J. Solution Chem.* **1997**, *26*, 877–888.

(28) Millero, F. J.; Ward, G. K.; Chetirkin, P. V. *J. Acoust. Soc. Am.* **1977**, *61*, 1492–1498.

(29) Lo Surdo, A.; Millero, F. J. *J. Phys. Chem.* **1980**, *84*, 710–715.

to a release of electrostricted water, because its  $\Delta V/\Delta K_S$  ratio is equal to  $0.35 \times 10^4$ .<sup>29,33,34</sup> To estimate the hydration contribution for the folding of the oligonucleotide into the  $\text{Sr}^{2+}$ -aptamer complex, we have adjusted the above parameters to take into account the coordination number of  $\text{Sr}^{2+}$  in this complex. This estimation yields a volume effect of  $-75 \text{ cm}^3/\text{mol}$  and a compressibility effect of  $-62 \times 10^{-4} \text{ cm}^3/\text{mol}\cdot\text{bar}$ ; the negative signs of these parameters show an overall uptake of water molecules. The resulting empirical  $\Delta V/\Delta K_S$  ratio<sup>34</sup> of  $1.2 \times 10^4 \text{ bar}$  suggests an uptake of hydrophobic water. This water may well be immobilized on the surface of the complex and around the constrained loops.

**Thermodynamic Profiles for the Formation of G-quadruplexes with  $\text{K}^+$  and  $\text{Sr}^{2+}$ .** Complete thermodynamic profiles for the formation of the  $\text{K}^+$ -aptamer and  $\text{Sr}^{2+}$ -aptamer complexes at a comparable ionic strength and 20 °C are presented in Table 2. The favorable  $\Delta G^\circ$  terms are similar in magnitude and result from the characteristic compensation of a favorable enthalpy term with an unfavorable entropy term. The favorable enthalpy term is the result of an exothermic heat from the stacking of two G-quartets that overrides the endothermic contribution of the release of electrostricted water from the cation. The endothermic contributions of disrupting base-base stacking interactions of the single strands are considered negligible, because the unfolding heats are similar in magnitude to the isothermal heats for both cation-aptamer complexes. The unfavorable entropy term results from contributions of the ordering of both a single strand and cation upon folding into a G-quadruplex and the overall immobilization of hydrophobic water by the complex. However, the magnitude of the enthalpy-entropy compensation is larger for the  $\text{K}^+$ -aptamer complex; the enthalpy term is more favorable (by  $-8.9 \text{ kcal/mol}$ ) despite its lower  $T_M$  (by  $\sim 18 \text{ }^\circ\text{C}$ ). This enthalpy difference may be explained in terms of several contributions: the hydration state of the free cations, yielding a differential release of water upon binding to the oligonucleotide; differential hydration of the cation-aptamer complexes; and different base-stacking contributions of the complexes.

To estimate these hydration contributions, we need to consider the dehydration effects of cations and O atoms upon coordination of the cation to eight O6 atoms of guanine and the hydration effects of quadruplex formation. The dehydration effects of each cation and O atoms are estimated using the molar compressibility values of  $28 \times 10^{-4} \text{ cm}^3/\text{mol}\cdot\text{bar}$  ( $\text{K}^+$ ),<sup>28,29</sup>  $75 \times 10^{-4} \text{ cm}^3/\text{mol}\cdot\text{bar}$  ( $\text{Sr}^{2+}$ ),<sup>29</sup> and  $10 \times 10^{-4} \text{ cm}^3/\text{mol}\cdot\text{bar}$  (O),<sup>35</sup> and the change in adiabatic compressibility of  $8.1 \times 10^{-4} \text{ cm}^3/\text{mol}\cdot\text{bar}$  for the transfer of water from the hydration shell of the ion to the bulk state.<sup>33</sup> These estimations yield overall dehydration effects of  $\sim 3$  electrostricted water molecules for  $\text{K}^+$ ,  $\sim 9$  for  $\text{Sr}^{2+}$ , and 1 water molecule per O atom. Because the hydration contribution of the single strand (in the  $\text{Cs}^+$  form) is similar for each reaction,  $\text{Sr}^{2+}$  would yield a higher release of six electrostricted water molecules. The hydration contribution for the rearrangement of a single-strand into a G-quadruplex is estimated from the experimental compressibility terms of Table 2. These compressibility values were corrected by the compressibility of the dehydration of cations and oxygen groups of

guanine to yield  $-9.5 \times 10^{-4} \text{ cm}^3/\text{mol}\cdot\text{bar}$  ( $\text{K}^+$  complex) and  $-46.6 \times 10^{-4} \text{ cm}^3/\text{mol}\cdot\text{bar}$  ( $\text{Sr}^{2+}$  complex). The uptake of hydrophobic water by each complex is estimated by dividing these values by the compressibility of water when immobilized around polar and nonpolar groups, assumed to be equal to  $-3.2 \times 10^{-4} \text{ cm}^3/\text{mol}\cdot\text{bar}$ .<sup>36</sup> This exercise yields an immobilization of  $\sim 3$  and  $\sim 15$  hydrophobic water molecules around the  $\text{K}^+$  and  $\text{Sr}^{2+}$  complexes, respectively, reflecting differences in the actual structure of complexes that resulted in different exposures of polar and nonpolar groups.

In terms of enthalpy contributions and relative to the formation of the  $\text{K}^+$ -aptamer complex, the differential dehydration effect of  $\text{Sr}^{2+}$  ions (6 electrostricted waters) corresponds to an endothermic heat contribution of  $\sim 1.8 \text{ kcal}$ ;<sup>37</sup> therefore, the remaining differential heat of  $7.1 \text{ kcal/mol}$  is due to differences in the stacking of G-quartets and/or endothermic contributions of the differential immobilization of 12 hydrophobic waters on the surface of the  $\text{Sr}^{2+}$  complex. We speculate that, depending on the extent of stacking interactions, the additional uptake of hydrophobic waters by the  $\text{Sr}^{2+}$  complex contributes to an endothermic heat ranging from 0 kcal/mol to 0.6 kcal/mol.

### Concluding Remarks

We initially used CD spectroscopy and UV melting techniques to determine the conformation and unfolding thermodynamics of G-quadruplexes with a variety of monovalent and divalent metal ions. The CD spectra and melting profiles as a function of strand concentration showed that  $\text{K}^+$ ,  $\text{Rb}^+$ ,  $\text{NH}_4^+$ ,  $\text{Sr}^{2+}$ , and  $\text{Ba}^{2+}$  are able to form stable intramolecular cation-aptamer complexes at temperatures above 25 °C. The cations  $\text{Li}^+$ ,  $\text{Na}^+$ ,  $\text{Cs}^+$ ,  $\text{Mg}^{2+}$ , and  $\text{Ca}^{2+}$  form weaker complexes at very low temperatures. These results have been rationalized in terms of their ionic radii; cations with an ionic radius in the range 1.3–1.5 Å fit well within the two G-quartets of the complex, while the other cations cannot. DSC and ITC techniques were used to characterize the unfolding and folding of cation-aptamer complexes with  $\text{K}^+$ ,  $\text{Rb}^+$ ,  $\text{NH}_4^+$ ,  $\text{Sr}^{2+}$ , and  $\text{Ba}^{2+}$ . The heat for the unfolding of each complex is in excellent agreement with the folding heat of isothermal titration experiments, indicating negligible contributions from base stacking interactions of the single strands. We have further characterized the hydration contributions for the formation of G-quadruplexes with  $\text{K}^+$  and  $\text{Sr}^{2+}$  using density and acoustical techniques. The overall thermodynamics parameters showed that the  $\text{Sr}^{2+}$ -aptamer complex unfolds with a higher transition temperature and lower endothermic heat, but its favorable formation (in terms of  $\Delta G^\circ$ ) is comparable to that of the  $\text{K}^+$ -aptamer complex. The overall hydration effects of complex formation yielded two main contributions, dehydration of both cations and guanine O6 atomic groups and the water uptake upon folding of a single strand into a G-quadruplex structure.

**Acknowledgment.** This work was supported by Grant GM42223 and Shared Instrumentation Grant S10 RR13660 from the National Institutes of Health.

JA010008O

(36) Kharakoz, D. P.; Marky, L. A. Manuscript in preparation. The compressibility of water around polar and nonpolar groups was estimated from acoustical investigations of the hydration of small sugar molecules, such as inositol, glucose, and mannitol.

(37) Gasan, A. I.; Maleev, V. Ya.; Semenov, M. A. *Stud. Biophys.* **1990**, *136*, 171–178.

(33) Millero, F. J.; Ward, G. K.; Lepple, F. K.; Hoff, E. V. *J. Phys. Chem.* **1974**, *78*, 1636–1643.

(34) Kankia, B. I.; Marky, L. A. *J. Phys. Chem.* **1999**, *103*, 8759–8767.

(35) Buckin, V. A.; Kankiya, B. I.; Kazaryan, R. L. *Biophys. Chem.* **1989**, *34*, 211–223.